

## Nicorandil inhibits TLR4/MyD88/NF- $\kappa$ B/NLRP3 signaling pathway to reduce pyroptosis in rats with myocardial infarction

Feng Chen<sup>1</sup>, Zhi-Qing Chen<sup>2</sup>, Gui-Ling Zhong<sup>2</sup> and Ji-Jin Zhu<sup>1,2</sup> 

<sup>1</sup>Department of Emergency, Guangxi Medical University First Affiliated Hospital, Nanning 530021, China; <sup>2</sup>Department of Cardiology, Guangxi Medical University First Affiliated Hospital, Nanning 530021, China  
Corresponding author: Ji-Jin Zhu. Email: Zhujijin63@163.com

### Impact statement

Myocardial infarction (MI) has high morbidity and mortality worldwide. However, the current protective methods for heart function after MI are still limited, and the mechanism of the cardioprotective effect of nicorandil remains unclear. This study demonstrates that nicorandil can ameliorate cardiac function by activating  $K_{ATP}$  channels, and by attenuating MI-induced pyroptosis by blocking the signaling of TLR4/MyD88/NF- $\kappa$ B/NLRP3. This suggests mechanisms by which nicorandil protects against myocardial injury caused by MI, and may impact the prevention and treatment of MI.

### Abstract

Pyroptosis is an inflammatory cell death that regulates cardiomyocyte loss after myocardial infarction. Reports indicate that nicorandil has a strong anti-inflammatory effect and protects the myocardium from myocardial infarction. However, its relationship with pyroptosis is largely unreported. Here, we investigated to influence and mechanism of action of nicorandil on cardiomyocyte pyroptosis. Forty Sprague Dawley rats were randomly assigned to sham, MI, MI + nicorandil, and MI + nicorandil + TAK242 groups (10 per group). Myocardial infarction modeling was performed through ligation of the anterior descending branch of the left coronary artery. The function of cardiac was evaluated through echocardiography, detection of myocardial adenine nucleotides, cTnl, LDH, TTC, and HE staining. Moreover, we used qRT-PCR, immunohistochemistry, and Western blotting to examine the expression of pyroptosis-related molecules and the inflam-

masome pathway of TLR4/MyD88/NF- $\kappa$ B/NLRP3. Myocardial infarction caused the activation of GSDMD, aggravated myocardial injury, and triggered cardiac dysfunction. Myocardial infarction induced pyroptotic cell death, manifested as upregulation in mRNA and protein levels associated with pyroptosis, including caspase-1 cleavage and increased expression of IL-1 $\beta$  and IL-18. These changes were mitigated by nicorandil. The achieved data implicate that myocardial infarction induces pyroptosis via the TLR4/MyD88/NF- $\kappa$ B/NLRP3 pathway, which can be inhibited by nicorandil pretreatment. Therefore, nicorandil exerts cardioprotective effects by activating  $K_{ATP}$  channels, and at least in part through inhibition of the TLR4/MyD88/NF- $\kappa$ B/NLRP3 pathway to reduce myocardial infarction-induced pyroptosis. As such, it is a potential therapy for ischemic heart disease.

**Keywords:** Nicorandil, myocardial infarction, gasdermin D, pyroptosis, myocardial injury, TLR4/MyD88/NF- $\kappa$ B/NLRP3 signaling pathway

*Experimental Biology and Medicine* 2021; 246: 1938–1947. DOI: 10.1177/15353702211013444

### Introduction

Myocardial infarction (MI) is a serious life-threatening cardiovascular event and results in high levels of mortality across the globe.<sup>1</sup> The present treatment for MI is primarily to reopen the infarcted vessels through percutaneous coronary intervention (PCI), increasing patient survival. However, the cardiomyocyte population is non-renewable and reperfusion after myocardial ischemia may trigger cell loss, potentially leading to heart failure (HF) in surviving

patients, thus imposing both disease and economic burdens on patients.<sup>2</sup> With the rapid improvement of living conditions and the aging of the world population, the incidence of cardiovascular events is likely to increase. The mechanism in preventing cardiomyocyte loss after MI has often been a fundamental focus by researchers. Therefore, in combination with reperfusion therapy, it is important to develop novel prevention and treatment approaches that

minimize myocardial cell death after MI, thereby limiting irreversible myocardial damage.

Pyroptosis was proposed by Cookson and Brennan as a new form of programmed cell death. Unlike apoptosis, its essence is the inflammatory death of cells, which might potentially be one of the mechanisms of cardiomyocyte loss.<sup>3</sup> Additionally, pyroptosis is characterized by cell perforation and leakage of intracellular pro-inflammatory factors and is dependent on the activation of pro-inflammatory caspases. In pyroptosis, activation of caspase-1 requires a pyroptosis-specific molecule, gasdermin D (GSDMD).<sup>4</sup> GSDMD is a caspase substrate and a key promoter of pyroptosis.<sup>5</sup> It is a pore-forming protein cleaved by the inflammatory caspase to produce N-terminal fragment oligomers (GSDMD-N) in the cytoplasm, which form 10–14 nm pores in the membrane of the cell allowing passage of IL-1 $\beta$  and IL-18.<sup>6</sup> It has been found that pyroptosis can induce the loss of cardiomyocytes in MI.<sup>7–9</sup> Nevertheless, the detailed regulatory mechanism requires further study.

Toll-like receptors (TLRs) are activated by cellular patterns including damage-associated molecular patterns (DAMPs). The primary TLRs expressed in cardiomyocytes include TLR2, TLR3, and TLR4<sup>10</sup> of which TLR4 is involved in myocardial injury caused by MI. Activation of TLR4 by DAMPs causes an inflammatory response in myocardial tissue, producing additional damage to the already damaged cardiomyocytes.<sup>11,12</sup> Previous reports have shown that myocardial inflammation is reduced by TLR4/Myd88/NF- $\kappa$ B pathway inhibition, improving cardiac function. For instance, inhibiting the expression of TLR4 reduces NLRP3-mediated inflammation and pro-inflammatory cytokines expression,<sup>13</sup> together with reducing the size of the myocardial infarction,<sup>14</sup> together with alleviating myocardial tissue remodeling and protecting cardiac function.<sup>15</sup> Therefore, to develop drugs that can effectively reduce the loss of cardiomyocytes and improve the prognosis of MI patients, it is necessary to investigate the involvement of the TLR4/Myd88/NF- $\kappa$ B/NLRP3 pathway in mediating pyroptotic cell death.

Nicorandil, an ATP-sensitive potassium channel opener, exhibits a cardioprotective effect by increasing coronary blood flow and reducing preload and afterload.<sup>16</sup> Studies have shown that nicorandil improves early functions and clinical problems in AMI patients,<sup>17</sup> and prevents long-term cardiovascular events and death in patients with ST-segment elevation MI.<sup>18</sup> Moreover, the application of nicorandil before PCI regulates postoperative inflammation and exerts myocardial protection.<sup>19,20</sup> However, besides dilating the coronary arteries, it is not known whether nicorandil improves heart function in other ways. The effects of nicorandil on pyroptosis and whether it can reduce pyroptotic death in cardiomyocytes are also not known. Therefore, this work explored the effect of nicorandil on myocardial pyroptosis and its molecular mechanism in a rat MI model.

## Materials and methods

### Animals

Animal experiments were accomplished according to the guidelines of the National Institutes of Health Guide for the Care and Use of Laboratory Animals and were confirmed through the Animal Ethics Committee of Guangxi Medical University. Forty male eight-week-old Sprague Dawley (SD) rats weighing 180–220 g were purchased from the Experimental Animal Center of Guangxi Medical University. The rats were maintained in a 12-h/12-h light/dark cycle with freely available water and food. Four groups of rats were randomly established ( $n = 10$  per group): the sham operation (Sham), MI, MI plus nicorandil (MI + Nic), and MI plus nicorandil plus TAK242 (MI + Nic + TAK242) groups. Based on previous findings, the MI + Nic group and MI + Nic + TAK242 group received 15 mg/kg nicorandil (Chugai Pharmaceutical Co., Japan) via intragastric administration once a day for seven consecutive days before MI modeling.<sup>21</sup> In the MI + Nic + TAK242 group, TAK242 (2 mg/kg, MedChem Express, Princeton, USA) was injected through the tail vein 30 min before MI modeling.<sup>13</sup>

### Rat MI modeling

MI modeling in the rats was produced as previously described via ligating the left anterior descending (LAD) coronary artery.<sup>22</sup> Rats were anesthetized 2% pentobarbital sodium (40 mg/kg; Merck, China) by intraperitoneal injection and received tracheal intubation and mechanical ventilation using a small animal ventilator. An incision was made from the edge of the left sternum between the third and fourth ribs to expose the left chest cavity before ligation of the LAD using a 6-0 suture approximately 2 mm from the start of the artery. Successful occlusion of the coronary artery was confirmed by the color change from red to white in the left ventricular wall and apex. The sham group underwent a similar procedure without ligation of the LAD.

### Cardiac function evaluation

Echocardiography was performed 72 h after the operation using a 7500 ultrasonic instrument from Hewlett-Packard Sonos with a 12.0 MHz probe (Philips Technologies, USA) was used for echocardiography. The left ventricular fractional shortening (LVFS), left ventricular ejection fraction (LVEF), left ventricular end-systolic diameter (LVESd), and the left ventricular end-diastolic diameter (LVEDd) were determined. After the cardiac function assessment, blood was sampled from the abdominal aorta to separate the serum, and then the rats were euthanized to remove the heart. The atrium and right ventricle were removed, and the heart was processed under the ligation line based on different experimental requirements. Figure 1 shows the experimental protocol.

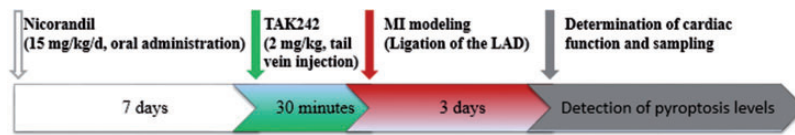


**Figure 1.** The timeline of the experimental protocol. (A color version of this figure is available in the online journal.)

**Table 1.** qRT-PCR primer sequences.

Gens	Forward primer (5'-3')	Reverse primer (5'-3')
TLR4	TATCGGTGGTCAGTGTGCTT	CTCGTTTCTCACCCAGTCCT
MyD88	AACTGAAGGACCGCATCGAG	AGCAGATGAAGGCGTCGAAA
NF- $\kappa$ B	GATCGCCACCGGATTGAAGA	CTCGGAAGGCACAGCAATA
NLRP3	CTCGCATTGGTTCTGAGCTC	AGTAAGGCCGGAATTCACCA
ASC	GCTGAGCAGCTGCAAAAGAT	GCAATGAGTGCCTTGCCTGTG
Caspase-1	GGAGCTTCAGTCAGGTCCATC	ATGCGCCACCTTCTTTGTTC
GSDMD	CTGGGAGATCATGCAACGTG	TCACCATCTTCTCCGGCTT
IL-18	TGCTCATCATGCTGTTCTGC	AGCCAAGAATCTCCGTAGCA
IL-1 $\beta$	GGGATGATGACGACCTGCTA	TGTGTTGCTTGTCTCTCCT
GAPDH	TTTGAGGGTGCAGCGAACTT	ACAGCAACAGGGTGGTGGAC

### Infarct size measurement

The frozen heart tissue was sectioned (1 mm sections) and stained with 2% 2,3,5-triphenyl tetrazolium chloride (TTC; Solarbio) at 37°C in the dark for 15 min before fixation with 4% formaldehyde solution for 15 min. Finally, the infarct size was quantified by ImageJ software (NIH).

### Myocardial adenine nucleotides assay

Myocardial ATP, ADP, and AMP were assayed by commercial detection kits (mlbio Biotechnology Co., Shanghai, China) conforming to the instructions of the kit. Briefly, 30 mg of myocardial tissue was collected and homogenized in 400  $\mu$ L of adenine nucleotide lysis buffer. The lysed material was centrifuged for 5 min at 4°C at 12,000g, and the supernatant was retained. Twenty microliters of supernatant were then added together with 100  $\mu$ L adenine nucleotide working solution to the wells of a 96-well plate, and the relative light unit value was measured with a luminometer. The concentrations of adenine nucleotides were determined from comparison with a standard curve.

### Determination of serum lactate dehydrogenase, cardiac troponin I, and inflammatory cytokines

Specific ELISA kits (Bioswamp, Wuhan, China) were utilized to assess the concentrations of cTnI, IL-1 $\beta$ , and IL-18 in rat sera, while LDH was measured by an automatic biochemical analyzer (Roche, Inc., Switzerland).

### Histological staining and immunohistochemical staining

Animal hearts were fixed (4% paraformaldehyde) and placed in paraffin. Five-micrometer sections were stained by using hematoxylin and eosin (HE) and GSDMD and NLRP3 immunohistochemical staining using anti-GSDMD (#93709, Cell Signaling Technologies, Danvers, MA, USA) and anti-NLRP3 (ab214185, Abcam,

Cambridge, UK) monoclonal antibodies. Images were observed with an Olympus FV300 confocal laser scanning microscope (Olympus, Japan).

### Quantitative real-time PCR

The extraction of total RNA was performed from myocardia with the TRIzol reagent (Invitrogen, Waltham, MA, USA), and the RNA concentration was determined by spectrophotometry. Then, reverse transcription was performed using reverse transcription kits (Takara, Japan) following the manufacturer's instructions to obtain cDNA. Next, the cDNA was amplified by qRT-PCR using the SYBR Green I PCR kit (TaKaRa, Japan). Reactions were conducted on the system of ABI PRISM 7500 (Applied BioSystems, Waltham, MA, USA). Table 1 illustrates the primer sequences. The internal reference was GAPDH. mRNA expression of MyD88, NF- $\kappa$ B, TLR4, NLRP3, caspase-1, ASC, GSDMD, IL-18, and IL-1 $\beta$  was quantified according to the  $2^{-\Delta\Delta Ct}$  approach.

### Western blot

Myocardial cells were lysed in a buffer containing 1% protease inhibitors, and the total protein concentration ascertained utilizing a bicinchoninic acid kit (Beyotime, China). Proteins were separated on 10% SDS-PAGE and blotted onto PVDF membranes (Millipore, Atlanta, GA, US). Following the blocking with 5% fat-free milk (1 h at room temperature), the incubation of the membranes was done with primary antibodies (anti-TLR4, MyD88, NF- $\kappa$ B p65, NLRP3, ASC, cleaved caspase-1, GSDMD, mature-IL-1 $\beta$ , mature-IL-18, and  $\beta$ -actin) at 4°C overnight. The anti-TLR4 (ab95562), MyD88 (ab219413), NF- $\kappa$ B p65 (ab16502), mature-IL-1 $\beta$  (ab200478), and mature-IL-18 (ab191860) primary antibodies were purchased from Abcam, while anti-ASC (#13833), cleaved caspase-1 (#89332), and  $\beta$ -actin (#3700) antibodies were from Cell Signaling Technologies. Membranes were then incubated with an HRP-conjugated

secondary antibody (sc-2357, sc-516102, Santa Cruz Biotechnology, Dallas, USA) for 2 h at room temperature. Finally, the washed membranes were evaluated for the protein signals with the enhanced chemiluminescence detection system. ImageJ computer program was utilized to assess the band intensities.

### Statistical analysis

All data were expressed as mean  $\pm$  standard deviation, and SPSS 17.0 and GraphPad Prism 8.0 were utilized for statistical analysis and graphing. The Student's *t*-test was utilized for the comparison of two groups, and one-way investigation of variance was utilized for the comparison of several groups. Each measurement was repeated at least three times, and a *P*-value  $< 0.05$  was regarded to be statistically significant.

## Results

### TLR4 and GSDMD expression is up-regulated in myocardia after MI

To explore the relationship between pyroptosis and MI, the expression of GSDMD, a key executor of pyroptosis, was determined in the myocardia. The expression of both GSDMD mRNA and GSDMD-N protein was enhanced in the MI group. Moreover, the expression of both interleukins was also elevated, suggesting an increase in pyroptosis in the injured myocardium. TLR4 and MyD88 also showed increased expression in the MI myocardium (Figure 2). These results indicate that MI-induced cardiomyocyte pyroptosis may occur through activation of the TLR4/MyD88 pathway.

### Nicorandil alleviates myocardial injury and improves cardiac function in MI rats

cTnI and LDH concentrations in sera were used to reflect damage to cardiomyocytes. The results showed that the

serum cTnI concentrations of the sham, MI, MI + Nic, and MI + Nic + TAK242 groups were  $0.18 \pm 0.04$ ,  $0.88 \pm 0.02$ ,  $0.68 \pm 0.10$ , and  $0.60 \pm 0.11$  ng/mL, respectively. The serum LDH concentrations of the sham, MI, MI + Nic, and MI + Nic + TAK242 groups were  $258.80 \pm 72.34$ ,  $1560.80 \pm 168.36$ ,  $1054.80 \pm 64.29$ , and  $939.00 \pm 110.54$  U/L, respectively. Figure 3(a) and (b) shows the serum concentrations of cTnI and LDH in the model group to be significantly higher and decreasing after Nic administration ( $P < 0.01$ ). Furthermore, ultrasound evaluation of rats' cardiac function (Figure 3(c)) showed that, in contrast to the sham group, the LVEF and LVFS values in the MI group were reduced, while the LVESd and LVEDd were increased ( $P < 0.01$ ), indicating left ventricular systolic dysfunction. However, unlike the untreated group, the cardiac dysfunction of MI rats was improved after nicorandil treatment, demonstrated by elevated LVEF and LVFS and decreased LVESd and LVEDd values ( $P < 0.01$ ) (Figure 3(d) to (g)).

### Nicorandil reduces myocardial infarction size and improves cardiomyocyte morphology

The infarct size was measured to further determine the effects of nicorandil on myocardial injury. As shown in Figure 4(a) and (b), the myocardial infarct size of the sham, MI, MI + Nic, and MI + Nic + TAK242 groups were 0,  $58.42 \pm 5.64$ ,  $23.49 \pm 6.21$ , and  $16.19 \pm 3.84$ , respectively, indicating significantly decreased infarct sizes after nicorandil administration ( $P < 0.01$ ). The morphological changes of cardiomyocytes were observed by HE staining. Cardiomyocytes in the sham group were intact with normal morphology, while in the MI group, the cells showed swelling with disintegrating nuclei. Inflammatory cells and lysed erythrocytes were also seen. Tissue sections from the Nic group contained significantly fewer swollen cells than the MI group (Figure 4(c)).

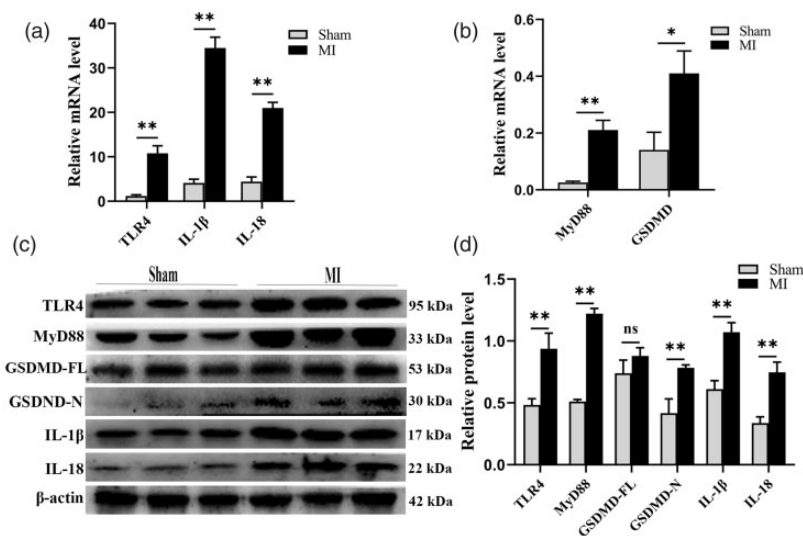


**Figure 2.** Increased expression of key executive molecules of pyroptosis after MI. (a–b) Comparison of mRNAs for TLR4, MyD88, GSDMD, IL-1 $\beta$ , and IL-18 between the MI and sham groups. (c) Representative Western blot bands of TLR4, MyD88, GSDMD-FL, GSDMD-N, IL-1 $\beta$ , and IL-18. (d) Comparison of protein expression levels between the MI and sham groups. The loading control was  $\beta$ -actin.  $n = 3$  per group. \* $P < 0.05$ , \*\* $P < 0.01$ , and ns means no statistical difference.

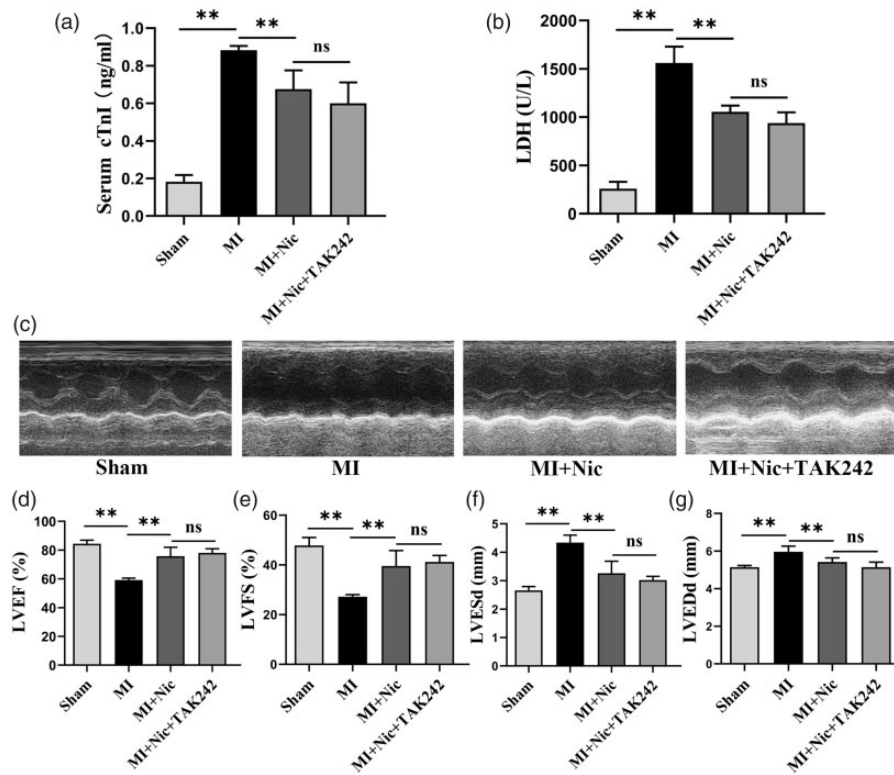


**Figure 3.** Nicorandil pretreatment attenuates cardiomyocyte injury and improves cardiac function after MI. (a–b) The level of cTnI and LDH in serum. (c) Representative M-mode images of each group. (d–g) LVEF, LVFS, LVESd, and LVEDd in each group.  $n = 5$  per group. \* $P < 0.05$ , \*\* $P < 0.01$ , and ns indicates no significant difference.

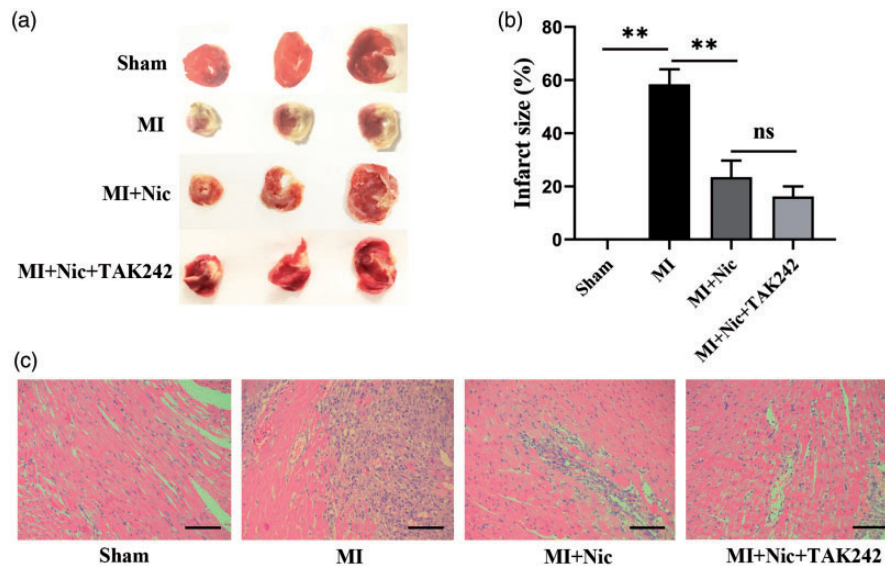


**Figure 4.** Nicorandil reduces infarct size and improves cardiomyocyte morphology. (a) Representative TTC staining pictures. (b) The percentage of infarct area in the groups. (c) Representative HE-stained myocardial sections from each group. Scale bar = 100 μm.  $n = 3$  per group. \* $P < 0.05$ , \*\* $P < 0.01$ , and ns indicates no significant difference. (A color version of this figure is available in the online journal.)

### Nicorandil pretreatment increases the adenine nucleotides in myocardia of MI rats

As described by Garlid *et al.*,<sup>23</sup> activation of the  $K_{ATP}$  potassium channel conserves ATP during cardiac ischemia. Since nicorandil is an opener of  $K_{ATP}$ , we assessed the level of  $K_{ATP}$  activation by determining the concentration of myocardial adenine nucleotides (ATP, ADP, and AMP),

followed by exploration of the cardioprotective mechanisms of nicorandil. It was found that compared with the sham group, MI clearly reduced myocardial ATP, ADP, and AMP concentrations. Similarly, the ATP/ADP ratio and total adenine nucleotide levels were also decreased. What was interesting, however, was that the adenine nucleotides in myocardial tissue after nicorandil pretreatment were

**Table 2.** Changes in ATP, ADP, AMP, ATP/ADP ratio, and total adenine nucleotides contents.

Groups	ATP ( $\mu\text{mol/L}$ )	ADP ( $\mu\text{mol/L}$ )	AMP ( $\mu\text{mol/L}$ )	ATP/ADP ratio	Total adenine nucleotides ( $\mu\text{mol/L}$ )
Sham	13.50 $\pm$ 1.22	9.49 $\pm$ 0.42	3.71 $\pm$ 1.09	1.42 $\pm$ 0.09	26.69 $\pm$ 0.65
MI	5.23 $\pm$ 0.31 <sup>a</sup>	5.38 $\pm$ 0.48 <sup>a</sup>	0.17 $\pm$ 0.06 <sup>a</sup>	0.98 $\pm$ 0.15 <sup>a</sup>	10.78 $\pm$ 0.20 <sup>a</sup>
MI + Nic	9.06 $\pm$ 0.73 <sup>b</sup>	7.25 $\pm$ 0.08 <sup>b</sup>	1.44 $\pm$ 0.61 <sup>b</sup>	1.25 $\pm$ 0.10 <sup>b</sup>	17.74 $\pm$ 0.99 <sup>b</sup>
MI + Nic + TAK242	10.41 $\pm$ 0.95 <sup>ns</sup>	7.57 $\pm$ 0.36 <sup>ns</sup>	1.76 $\pm$ 0.47 <sup>ns</sup>	1.37 $\pm$ 0.06 <sup>ns</sup>	19.74 $\pm$ 0.90 <sup>c</sup>

ATP: adenosine triphosphate; ADP: adenosine diphosphate; AMP: adenosine monophosphate; MI: myocardial infarction; Nic: nicorandil.

Note: Note: Nicorandil pretreatment increases the adenine nucleotides in myocardium of MI rats. The results are presented as mean  $\pm$  standard deviation.  $n = 3$  per group.

<sup>a</sup> $P < 0.05$  vs. Sham; <sup>b</sup> $P < 0.05$  vs. MI; <sup>c</sup> $P < 0.05$  vs. MI + TAK242; <sup>ns</sup> $P > 0.05$  vs. MI + TAK242.

significantly elevated in comparison with the MI group (Table 2). This result agrees with the findings of a previous study,<sup>24</sup> and demonstrated that nicorandil pretreatment increased the ATP content by opening  $K_{ATP}$  channels during MI, which assisted the maintenance of the mitochondrial oxygen consumption rate under hypoxic conditions.

### Nicorandil protects cardiomyocytes from MI-induced pyroptosis

To study the influence of nicorandil on myocardial pyroptosis after ischemia, its effects on the expression of pyroptosis-associated proteins were investigated. The mRNA expression of all these genes was found to be increased in the MI group ( $P < 0.01$ ) (Figure 5(a) to (d)). The levels of protein, including GSDMD-N and cleaved caspase-1, were also significantly increased ( $P < 0.01$ ) (Figure 5(e) and (f)). The immunohistochemical results showed GSDMD expression to be enhanced in MI (Figure 5(g)). Additionally, ELISA data indicated that in the MI group, IL-18 and IL-1 $\beta$  expression was considerably enhanced ( $P < 0.01$ ). The cytokine levels in the sham, MI, MI + Nic, and MI + Nic + TAK242 sera were 19.26  $\pm$  1.67, 85.41  $\pm$  8.35, 64.47  $\pm$  9.15, 54.14  $\pm$  13.11, and 31.58  $\pm$  4.37, 147.89  $\pm$  15.33, 95.37  $\pm$  5.48, 81.12  $\pm$  11.58 pg/mL, respectively (Figure 5(h) and (i)). Notably, nicorandil pretreatment significantly prevented these effects, confirming that nicorandil exhibits an inhibitory effect on MI-induced pyroptotic cell death.

### Nicorandil inhibits pyroptosis through the TLR4/MyD88/NF- $\kappa$ B/NLRP3 pathway

The rats were pretreated with a TLR4-specific inhibitor (TAK242) and the levels of TLR4, MyD88, NF- $\kappa$ B, NLRP3, and ASC were determined to establish the relationship between the inhibition of MI-induced cardiomyocyte pyroptosis by nicorandil and the TLR4/MyD88/NF- $\kappa$ B/NLRP3 pathway. In the Nic group, expression, both mRNA and protein, of the above indicators was significantly lower than the MI group, as shown in Figure 6(a) to (g) ( $P < 0.01$ ). However, the combination of TAK242 and nicorandil did not improve the influence of nicorandil ( $P > 0.05$ ). NLRP3 is implicated in caspase-1 activation, which cleaves GSDMD to produce N-terminal fragments, inducing pyroptosis.<sup>25</sup> Moreover, immunohistochemical detection of myocardial NLRP3 showed that after pretreatment with Nic and TAK242, the NLRP3 level in myocardial

tissue was not clearly downregulated compared to Nic alone (Figure 6(h)). These results suggest that nicorandil inhibits MI-induced cardiomyocyte pyroptosis, at least in part, through the signaling of TLR4/MyD88/NF- $\kappa$ B/NLRP3.

## Discussion

Our study explored the effect of nicorandil on cardiomyocyte pyroptosis in a rat MI model and the potential mechanism involved. First, we observed that cardiomyocyte pyroptosis is a vital pathophysiological event in MI, resulting in a massive loss of cardiomyocytes, which are non-renewable cells, and eventually cardiac dysfunction. Secondly, nicorandil pretreatment could significantly increase the levels of adenine nucleotides, reduce the size of the MI, and improve cardiac insufficiency. In terms of the mechanism, nicorandil activated the  $K_{ATP}$  channel, and blocked GSDMD activation *via* inhibiting the signaling of TLR4/MyD88/NF- $\kappa$ B/NLRP3. Moreover, it reduces the release of pro-inflammatory cytokines thereby significantly inhibiting pyroptotic cell death (Figure 7). The findings provide new evidence demonstrating the protective effect of nicorandil against myocardial ischemic diseases and offer new ideas for preventing and treating MI-induced cardiomyocyte loss, thus improving cardiac function. However, there are several remaining issues that warrant further studies.

Despite reperfusion therapy reducing the mortality of MI, both hypoxia and reoxygenation cause irreversible damage to cardiomyocytes. The damaged myocardium cannot regenerate and is replaced by scar tissue that is unable to produce myocardial contractions and ultimately leads to heart failure in survivors.<sup>26</sup> This shows that the primary cause of myocardial injury is cardiomyocyte death. Therefore, elucidating the specific mechanism of ischemia-hypoxia-induced cardiomyocyte loss is essential. Pyroptosis is an inflammation-mediated programmed cell death and is an important cause of cardiomyocyte loss after MI.<sup>7</sup> GSDMD, a pore-forming protein, is activated after being cleaved by activated caspase to produce GSDMD-N, transfers to the cell membrane, and executes pyroptosis by forming membrane pores to release the mature interleukins.<sup>27</sup> Reports indicate that during the pathogenesis of MI, NLRP3 activates pro-caspase-1 by forming an inflammatory complex with ASC, leading to cardiomyocyte death.<sup>8</sup> Furthermore, the activation of NLRP3 inflammasomes requires the response of toll-like receptors to DAMPs or

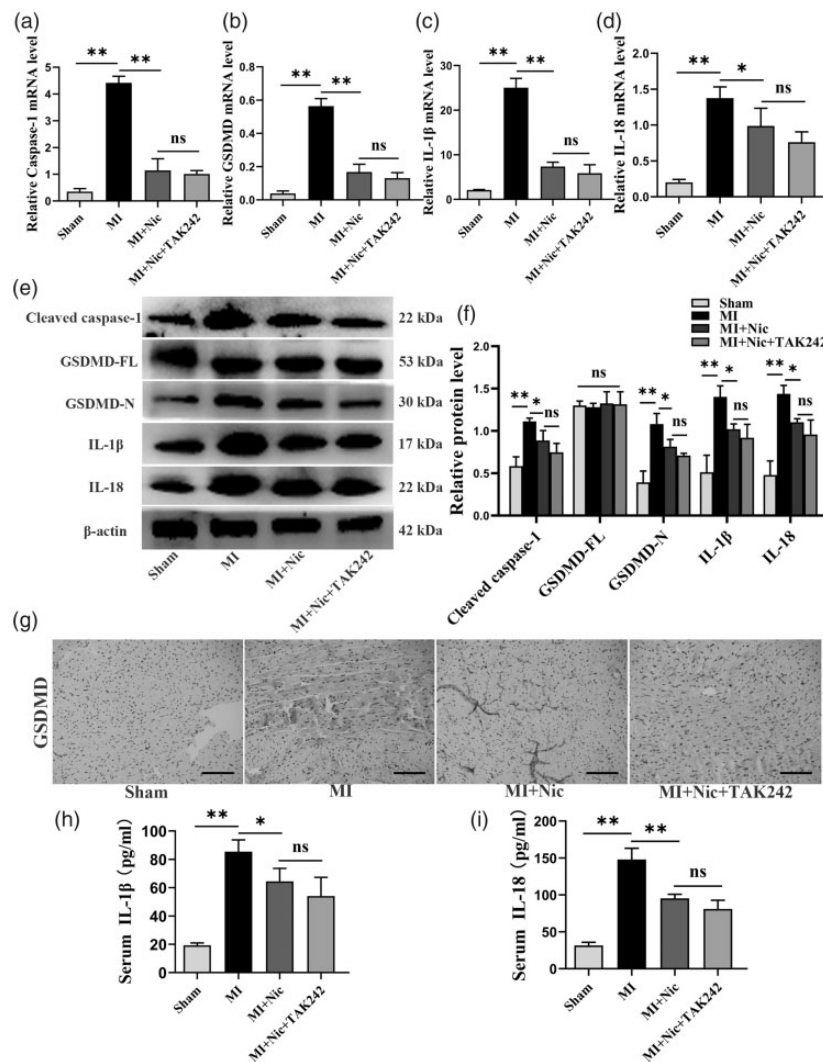


**Figure 5.** Nicorandil attenuates MI-induced pyroptosis of cardiomyocytes. (a–d) mRNA levels of caspase-1, GSDMD, IL-1 $\beta$ , and IL-18 in the groups. (e) Representative Western blot bands of cleaved caspase-1, GSDMD-FL, GSDMD-N, IL-1 $\beta$ , and IL-18. F, The relative expression levels of these proteins in each group.  $\beta$ -actin was utilized to normalize protein expression. (g) Representative GSDMD immunohistochemical staining pictures of each group. Scale bar = 100  $\mu$ m. (h–i) Serum IL-1 $\beta$ , and IL-18 levels of rats in each group.  $n = 3$  per group. \* $P < 0.05$ , \*\* $P < 0.01$ , and ns indicates no significant difference. (A color version of this figure is available in the online journal.)

pathogen-associated molecular patterns (PAMPs) and initiates the important step of recruiting MyD88 to activate NF- $\kappa$ B.<sup>28</sup> Of the toll-like receptors, TLR4 is the most widely studied and the most promising new target for the treatment of ischemic heart disease. Numerous reports have indicated that TLR4 is activated in ischemic heart disease, leading to upregulated expression of proinflammatory factors, causing additional damage to the already damaged myocardium.<sup>10,11</sup> Nonetheless, inhibiting TLR4 significantly reduces myocardial injury and improves cardiac function.<sup>13–15</sup>

Nicorandil is a  $K_{ATP}$  channel opener with nitrate function.<sup>17</sup> Although no evidence exists on the relationship between nicorandil and cell pyroptosis, several studies have shown that it protects cardiovascular functioning demonstrated.<sup>19,20,29</sup> Because the essence of pyroptosis is also inflammatory death, we speculate that nicorandil exhibits an inhibitory effect on MI-induced pyroptotic cell death. Moreover, its potential mechanism may be through

the opening of the  $K_{ATP}$  channels, as well as involving interference with TLR4/MyD88/NF- $\kappa$ B/NLRP3 signaling. Further investigation should explore the relationship between  $K_{ATP}$  channels and pyroptosis.

Here, myocardial injury and left ventricular systolic dysfunction occurred in rats after MI modeling, manifested by increased cTnI and LDH and decreased LVEF and LVFS values, as well as increased LVESd and LVEDd. These findings indicate that the establishment of the MI model was effective. Subsequently, we explored the expression of GSDMD, a key protein that induces pyroptosis, and confirmed that its expression was significantly up-regulated in MI. Further, we observed that the expression of other molecules related to pyroptosis was also up-regulated in MI. This indicates that pyroptosis occurs during the pathogenesis of MI. Secondly, we investigated the effects of nicorandil pretreatment on pyroptosis and cardiac function in MI rats. Unlike the MI group, the Nic-pretreated rats had less myocardial injury, smaller infarct size, improved cardiac

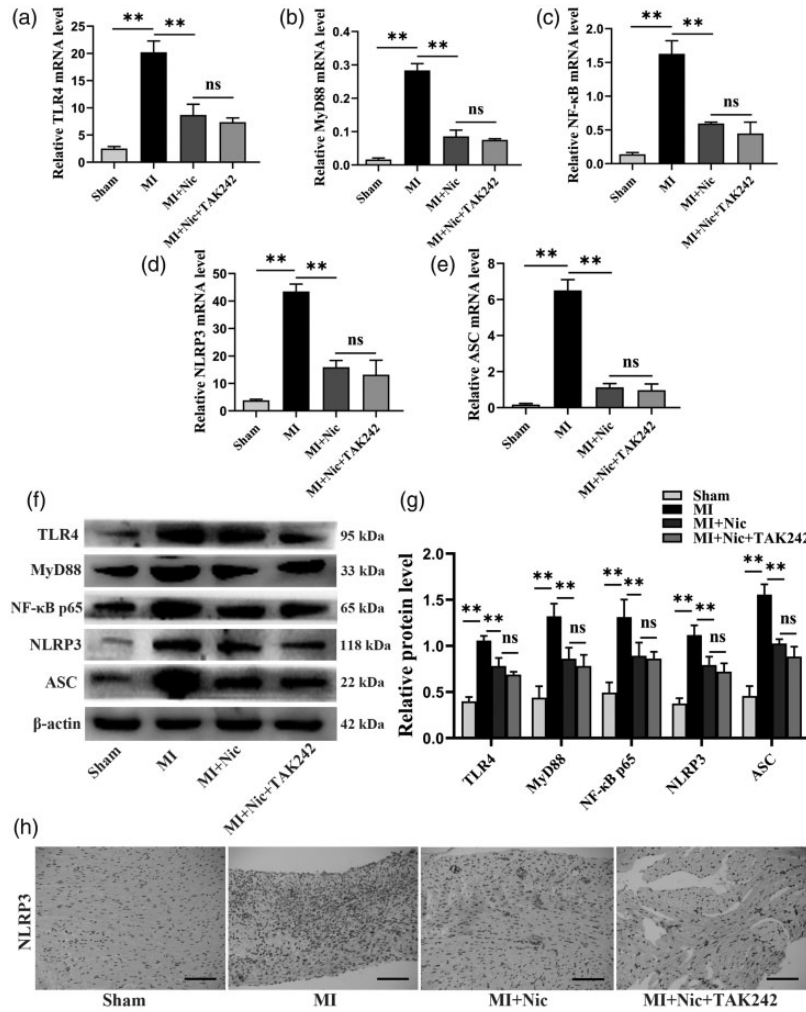


**Figure 6.** Nicorandil inhibits MI-induced pyroptosis through the TLR4/MyD88/NF-κB/NLRP3 signaling pathway. (a–e) The mRNA levels of TLR4, MyD88, NF-κB, NLRP3, and ASC in each group. (f) Representative Western blot bands of cleaved TLR4, MyD88, NF-κB p65, NLRP3, and ASC. (g) Relative protein expression levels in each group. β-actin was the loading control. (h) Representative NLRP3 immunohistochemical staining in each group. Scale bar = 100 μm. n = 3 per group. \*P < 0.05, \*\*P < 0.01, and ns represents no significant difference. (A color version of this figure is available in the online journal.)

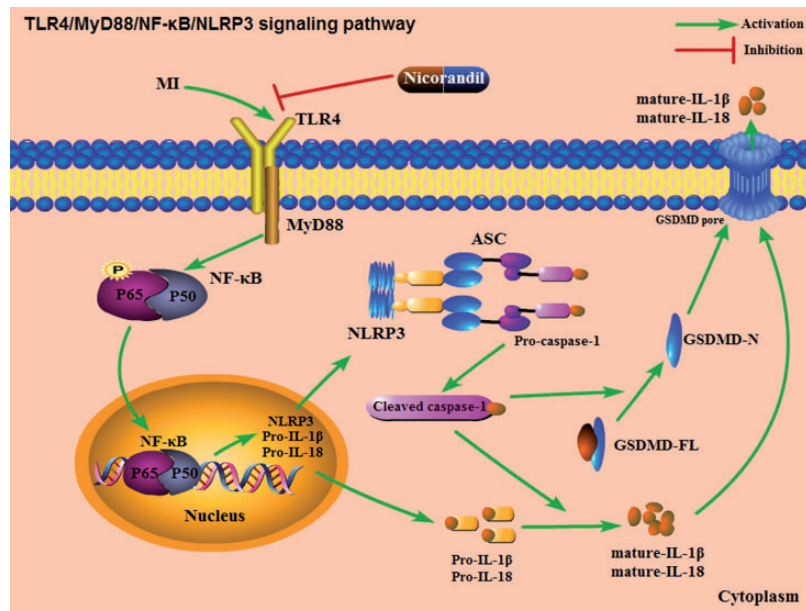


**Figure 7.** Schematic diagram of the potential molecular anti-pyroptotic mechanism of nicorandil via the TLR4/MyD88/NF-κB/NLRP3 pathway.

function, and reduced pyroptosis, demonstrated by decreased cTnI and LDH, increased adenine nucleotides, elevated LVEF and LVFS, and decreased LVESd and LVEDd, as well as downregulated expression of caspase-1, GSDMD, IL-1 $\beta$ , and IL-18. This suggests that nicorandil inhibits myocardial cell pyroptosis and improves the cardiac function of rats. Finally, we explored whether the TLR4/MyD88/NF- $\kappa$ B/NLRP3 signaling pathway was implicated within the protective effect of nicorandil on myocardial pyroptosis injury. We also found that nicorandil significantly inhibited the expression of TLR4, causing a down-regulation of the expression of its downstream target proteins. However, the combination of nicorandil and TAK242, a specific inhibitor of TLR4, did not further enhance the inhibition of TLR4 ( $P > 0.05$ ). We, therefore, conclude that nicorandil at least partially blocks TLR4/MyD88/NF- $\kappa$ B/NLRP3 signaling to attenuate myocardial pyroptosis in MI-induced myocardial injury, which may also involve the activation of  $K_{ATP}$  channels.

This work has a few limitations. First, we simulated MI by ligating the coronary artery. Although this physical occlusion method produces a pathophysiological response similar to atherosclerotic plaque embolism, the composition of atherosclerotic plaque is complex and has biological characteristics that can be altered under the influence of drugs, while physical occlusion is relatively less affected by drugs. Therefore, this is somewhat different from the actual MI situation. Secondly, the involvement of atypical pyroptosis signals or other forms of cell death cannot be excluded, which merits further study. Furthermore, the TLR4 inhibitor in the case of nicorandil intervention triggered an overlap of the two synergies; hence, it might be better to give agonists. Finally, the direct causal relationship between the expression of TLR4, MyD88, NF- $\kappa$ B, and NLRP3, as well as the relationship between the  $K_{ATP}$  channels and pyroptosis remained unconfirmed, and future research should determine the link between them.

## Conclusions

In conclusion, this study shows that nicorandil alleviates cardiomyocyte pyroptosis and enhances cardiac function in MI rats. The underlying mechanism involves, at least in part, the TLR4/MyD88/NF- $\kappa$ B/NLRP3 signaling pathway which could be associated with the activation of  $K_{ATP}$  channels. This might potentially be one of the vital mechanisms for the preventive application of nicorandil before PCI or the treatment of ischemic heart disease to improve the disease prognosis. Overall, nicorandil is an effective therapy for ischemic heart disease and is worth further consideration.

## AUTHORS' CONTRIBUTIONS

FC, ZQC, and GLZ conducted the experiments and data analysis. JJZ and FC participated in the design, interpretation of the study, wrote and reviewed critical revision of the article. All authors read and approved the final manuscript.

## DECLARATION OF CONFLICTING INTERESTS

The author(s) declared no potential conflicts of interest with respect to the research, authorship, and/or publication of this article.

## FUNDING

The author(s) disclosed receipt of the following financial support for the research, authorship, and/or publication of this article: This study was supported by the Natural Science Foundation of Guangxi (No. 2015GXNSFAA139156).

## ORCID iD

Ji-Jin Zhu  <https://orcid.org/0000-0001-6419-1350>

## REFERENCES

- Benjamin EJ, Blaha MJ, Chiuve SE, Cushman M, Das SR, Deo R, de Ferranti SD, Floyd J, Fornage M, Gillespie C, Isasi CR, Jimenez MC, Jordan LC, Judd SE, Lackland D, Lichtman JH, Lisabeth L, Liu S, Longenecker CT, Mackey RH, Matsushita K, Mozaffarian D, Mussolino ME, Nasir K, Neumar RW, Palaniappan L, Pandey DK, Thiagarajan RR, Reeves MJ, Ritchey M, Rodriguez CJ, Roth GA, Rosamond WD, Sasson C, Towfighi A, Tsao CW, Turner MB, Virani SS, Voeks JH, Willey JZ, Wilkins JT, Wu JH, Alger HM, Wong SS, Muntner P, American Heart Association Statistics Committee and Stroke Statistics Subcommittee. Heart disease and stroke statistics-2017 update: a report from the American Heart Association. *Circulation* 2017;**135**:e146-603
- Ibanez B, James S, Agewall S, Antunes MJ, Bucciarelli-Ducci C, Bueno H, Caforio ALP, Crea F, Goudevenos JA, Halvorsen S, Hindricks G, Kasrati A, Lenzen MJ, Prescott E, Roffi M, Valgimigli M, Varenhorst C, Vranckx P, Widimsky P, Group E. 2017 ESC guidelines for the management of acute myocardial infarction in patients presenting with ST-segment elevation: the task force for the management of acute myocardial infarction in patients presenting with ST-segment elevation of the European Society of Cardiology (ESC). *Eur Heart J* 2018;**39**:119-77
- Cookson BT, Brennan MA. Pro-inflammatory programmed cell death. *Trends Microbiol* 2001;**9**:113-4
- Shi J, Zhao Y, Wang K, Shi X, Wang Y, Huang H, Zhuang Y, Cai T, Wang F, Shao F. Cleavage of GSDMD by inflammatory caspases determines pyroptotic cell death. *Nature* 2015;**526**:660-5
- Sborgi L, Ruhl S, Mulvihill E, Pipercevic J, Heilig R, Stahlberg H, Farady CJ, Muller DJ, Broz P, Hiller S. GSDMD membrane pore formation constitutes the mechanism of pyroptotic cell death. *EMBO J* 2016;**35**:1766-78
- Ding J, Wang K, Liu W, She Y, Sun Q, Shi J, Sun H, Wang DC, Shao F. Pore-forming activity and structural autoinhibition of the gasdermin family. *Nature* 2016;**535**:111-6
- Mezzaroma E, Toldo S, Farkas D, Seropian IM, Van Tassell BW, Salloum FN, Kannan HR, Menna AC, Voelkel NF, Abbate A. The inflammasome promotes adverse cardiac remodeling following acute myocardial infarction in the mouse. *Proc Natl Acad Sci U S A* 2011;**108**:19725-30
- Bergsbaken T, Fink SL, Cookson BT. Pyroptosis: host cell death and inflammation. *Nat Rev Microbiol* 2009;**7**:99-109
- Frantz S. Targeted deletion of caspase-1 reduces early mortality and left ventricular dilatation following myocardial infarction. *J Mol Cell Cardiol* 2003;**35**:685-94
- Liu L, Wang Y, Cao ZY, Wang MM, Liu XM, Gao T, Hu QK, Yuan WJ, Lin L. Up-regulated TLR4 in cardiomyocytes exacerbates heart failure after long-term myocardial infarction. *J Cell Mol Med* 2015;**19**:2728-40
- Timmers L, Sluijter JP, van Keulen JK, Hoefler IE, Nederhoff MG, Goumans MJ, Doevendans PA, van Echteld CJ, Joles JA, Quax PH, Piek JJ, Pasterkamp G, de Kleijn DP. Toll-like receptor 4 mediates

- maladaptive left ventricular remodeling and impairs cardiac function after myocardial infarction. *Circ Res* 2008;**102**:257–64
12. Frantz S, Kobzik L, Kim YD, Fukazawa R, Medzhitov R, Lee RT, Kelly RA. Toll4 (TLR4) expression in cardiac myocytes in normal and failing myocardium. *J Clin Invest* 1999;**104**:271–80
  13. Su Q, Li L, Sun Y, Yang H, Ye Z, Zhao J. Effects of the TLR4/Myd88/NF-kappaB signaling pathway on NLRP3 inflammasome in coronary Microembolization-Induced myocardial injury. *Cell Physiol Biochem* 2018;**47**:1497–508
  14. Zhang J, Zhang J, Yu P, Chen M, Peng Q, Wang Z, Dong N. Remote ischaemic preconditioning and sevoflurane postconditioning synergistically protect rats from myocardial injury induced by ischemia and reperfusion partly via inhibition TLR4/MyD88/NF-kappaB signaling pathway. *Cell Physiol Biochem* 2017;**41**:22–32
  15. Yuan X, Deng Y, Guo X, Shang J, Zhu D, Liu H. Atorvastatin attenuates myocardial remodeling induced by chronic intermittent hypoxia in rats: partly involvement of TLR-4/MYD88 pathway. *Biochem Biophys Res Commun* 2014;**446**:292–7
  16. Group IS. Effect of nicorandil on coronary events in patients with stable angina: the impact of nicorandil in angina (IONA) randomised trial. *Lancet* 2002;**359**:1269–75
  17. Ito H, Taniyama Y, Iwakura K, Nishikawa N, Masuyama T, Kuzuya T, Hori M, Higashino Y, Fujii K, Minamino T. Intravenous nicorandil can preserve microvascular integrity and myocardial viability in patients with reperfused anterior wall myocardial infarction. *J Am Coll Cardiol* 1999;**33**:654–60
  18. Ishii H, Ichimiya S, Kanashiro M, Amano T, Imai K, Murohara T, Matsubara T. Impact of a single intravenous administration of nicorandil before reperfusion in patients with ST-segment-elevation myocardial infarction. *Circulation* 2005;**112**:1284–8
  19. Hu K, Wang X, Hu H, Xu Z, Zhang J, An G, Su G. Intracoronary application of nicorandil regulates the inflammatory response induced by percutaneous coronary intervention. *J Cell Mol Med* 2020;**24**:4863–70
  20. Isono T, Kamihata H, Sutani Y, Motohiro M, Yamamoto S, Kyoui S, Iharada Y, Kurimoto K, Hara K, Takahashi H, Iwasaka T. Nicorandil suppressed myocardial injury after percutaneous coronary intervention. *Int J Cardiol* 2008;**123**:123–8
  21. Su Q, Lv X, Sun Y, Ye Z, Kong B, Qin Z. Role of TLR4/MyD88/NF-kappaB signaling pathway in coronary microembolization-induced myocardial injury prevented and treated with nicorandil. *Biomed Pharmacother* 2018;**106**:776–84
  22. Hou Y, Huang C, Cai X, Zhao J, Guo W. Improvements in the establishment of a rat myocardial infarction model. *J Int Med Res* 2011;**39**:1284–92
  23. Garlid KD, Paucek P, Yarov-Yarovoy V, Murray HN, Darbenzio RB, D'Alonzo AJ, Lodge NJ, Smith MA, Grover GJ. Cardioprotective effect of diazoxide and its interaction with mitochondrial ATP-sensitive K<sup>+</sup> channels. Possible mechanism of cardioprotection. *Circ Res* 1997;**81**:1072–82
  24. Ahmed LA, Salem HA, Attia AS, Agha AM. Pharmacological preconditioning with nicorandil and pioglitazone attenuates myocardial ischemia/reperfusion injury in rats. *Eur J Pharmacol* 2011;**663**:51–8
  25. Man SM, Kanneganti TD. Gasdermin D: the long-awaited executioner of pyroptosis. *Cell Res* 2015;**25**:1183–4
  26. Cohn JN, Ferrari R, Sharpe N. Cardiac remodeling – concepts and clinical implications: a consensus paper from an international forum on cardiac remodeling. *J Am Coll Cardiol* 2000;**35**:569–82
  27. Liu X, Zhang Z, Ruan J, Pan Y, Magupalli VG, Wu H, Lieberman J. Inflammasome-activated gasdermin D causes pyroptosis by forming membrane pores. *Nature* 2016;**535**:153–8
  28. Afonina IS, Zhong Z, Karin M, Beyaert R. Limiting inflammation—the negative regulation of NF-kappaB and the NLRP3 inflammasome. *Nat Immunol* 2017;**18**:861–9
  29. Wang X, Pan J, Liu D, Zhang M, Li X, Tian J, Liu M, Jin T, An F. Nicorandil alleviates apoptosis in diabetic cardiomyopathy through PI3K/akt pathway. *J Cell Mol Med* 2019;**23**:5349–59

(Received January 15, 2021, Accepted April 9, 2021)